



OPEN

Expression of TXNIP is associated with angiogenesis and postoperative relapse of conventional renal cell carcinoma

Mate Meszaros¹, Maria Yusenko², Lilla Domonkos¹, Lehel Peterfi¹, Gyula Kovacs^{1,3}✉ & Daniel Banyai¹

One of the common mediator of tumour progression is the oxidative stress induced by inflammatory tumour microenvironment (TME). Activated fibroblasts, local and immune cells produce reactive oxygen species (ROS) supporting tumour cell proliferation and pave the way for metastatic tumour growth. TXNIP regulates ROS generation by inhibiting the antioxidative function of thioredoxin (TXN). The shift of TXNIP/TXN balance towards overexpression of TXNIP is associated with proliferation of endothelial cells during tumor angiogenesis. The oxidative stress activates the hypoxia inducible factor-1 (HIF-1), which plays an important role in the biology of conventional RCC (cRCC). Under oxydative stress TXNIP interacts with NLRP3 inflammasome leading to maturation and secretion of inflammatory cytokine IL1 β . To establish the role of TXNIP and downstream genes HIF1 α and IL1 β in the biology of cRCC, we have applied immunohistochemistry to multi-tissue arrays containing tumours of 691 patients without detectable metastases at the time of operation. We found that cRCC displaying a fine organised capillary network with nuclear translocation of TXNIP and expressing IL1 β have a good prognosis. In contrary, we showed a significant correlation between cytoplasmic TXNIP expression, inefficient vascularisation by unorganized and tortuous vessels causing tumour cell necrosis and postoperative tumour relapse of cRCC.

Conventional renal cell carcinoma (cRCC) makes up 80% of malignant kidney tumours. Approximately 40% of the patients with cRCC have a metastasis at the time of operation or will develop metastatic disease during the postoperative course of 5 years¹. Introducing modern imaging techniques resulted in a growing number of patients with incidentally detected small renal tumours confined to the kidney^{2,3}. However, approximately 15% of clinically localised tumours operated with curative intent develops metastasis within 5 years follow-up. Recent drug therapies can not cure the disease, but they may prolong the life of patients with metastatic disease^{4,5}. Therefore, it is a need for biomarkers to identify a group of patients with high risk of postoperative tumor relapse to be able to start adjuvant therapy as early as possible.

The inflammatory tumour microenvironment (TME) plays a crucial role in development and progression of malignant tumours^{6,7}. The TME comprises stromal cells, blood vessels, activated fibroblasts, extracellular matrix as well as reactive oxygen species (ROS) producing innate and adaptive immune cells^{8–10}. IL6, TGF β and TNF α expressed in TME generates ROS triggering cell proliferation and survival¹¹. ROS is also formed by NADPH oxidases, which can be activated by various growth factors^{12,13}. ROS generated by oxidative cellular stress play an important role in signalling pathways through AKT and ERK1/2 and activation of hypoxia inducible factor-1 (HIF-1)^{14,15}. Thioredoxin-interacting protein (TXNIP) contribute substantially to accumulation of intracellular ROS by inhibiting the antioxidative function of thioredoxin (TXN)¹⁶. TXNIP expression and elevated level of ROS is required for VEGF-mediated VEGFR2 activation and proliferation of endothelial cells during tumor angiogenesis^{17,18}. Under oxydative stress TXNIP interacts with NLRP3 inflammasome leading to maturation

¹Department of Urology, Medical School, University of Pecs, Pecs, Hungary. ²Institute of Biochemistry, University of Muenster, Muenster, Germany. ³Medical Faculty, Ruprecht-Karls-University, Heidelberg, Germany. ✉email: g.kovacs@gmx.de

and secretion of inflammatory cytokine IL1 β ^{19,20}. It was shown that IL1 β mediates epithelial to mesenchymal transition of proximal tubular cells of kidney²¹.

Controversial results have been published on TXNIP expression and tumour progression. High level of TXNIP expression was associated with a significantly shorter survival of patients with non-small cell lung cancer and invasive growth of hepatocellular carcinoma^{22,23}. On the other hands, lack or reduced expression of TXNIP in cancer cell lines, experimental mouse models as well as in tumour tissues suggested that TXNIP is a tumour suppressor gene^{24–30}. It has also been reported that decreased TXNIP RNA expression is associated with poor prognosis of patients with clear cell renal cell carcinoma³¹. To establish the role of TXNIP and downstream genes HIF1 α and IL1 β in the biology of cRCC, we have applied immunohistochemistry to tissue multi-arrays containing tumours of patients without detectable metastases at the time of operation.

Results

Expression of TXNIP in normal kidney. TXNIP showed a weak expression at the luminal surface of proximal tubular cells and a strong cytoplasmic expression in connecting and collecting duct cells in normal adult kidneys, whereas the loop of Henle and distal convoluted tubules were negative (data not shown). Vascular smooth muscle cells and endothelial cells of small kidney arteria displayed a weak TXNIP expression. We did not find nuclear TXNIP expression in normal adult kidney. No expression of HIF1 α and IL1 β has been seen in normal kidney tissue.

Expression of TXNIP in conventional RCC. Results of immunohistochemistry of 691 cRCC separated two groups of tumours. One group of 512 tumours (74%) without cytoplasmic expression of TXNIP (Fig. 1A), and the other group displaying medium or strong cytoplasmic TXNIP staining in 95 (14%) and 84 (12%) cases, respectively. (Fig. 1B). As the first Kaplan–Meier analysis revealed that patients with medium or strong cytoplasmic TXNIP expression have similar disease-free survival, we have evaluated the results of cytoplasmic TXNIP immunohistochemistry in correlation to clinical and pathological parameters as negative or positive.

Expression of IL1 β and HIF1 α in conventional RCC. We used the same series of TMA as for TXNIP immunohistochemistry. A granular cytoplasmic IL1 β expression has been seen in 601 of the 691 conventional RCCs (Fig. 1C), whereas 90 cases showed a negative immunoreaction with IL1 β antibody (Fig. 1D). We did not find HIF1 α expression in any of the tumour cells analysed in this study. Positive HIF1 α staining has been detected in some endothelial cells and in tumour infiltrating immune cells.

TXNIP expression in tumour microvessels. Irrespectively of positive or negative cytoplasmic expression in tumour cells TXNIP showed a strong expression in endothelial cells of the tumour stroma. In highly differentiated cRCC resembling the classic “Grawitz” tumour a fine network of TXNIP positive endothelial cells and tumour cells without TXNIP staining was seen (Fig. 2A). The overwhelming majority of endothelial cells displayed a nuclear TXNIP expression (Fig. 2B). In the second group of tumours with medium or high TXNIP expression in tumour cells only few vessels has been recognized. The majority of TXNIP positive tumours displayed unorganized, irregular or tortuous tumour vessels (Fig. 2C) as compared to those seen in well differentiated cRCC (Figs. 1A and 2A). Around small necrotic tumour areas tumour cells displayed strong cytoplasmic TXNIP immunoreaction (Fig. 2D). As vascular TXNIP expression has been detected in all tumours analysed in this cohort, we evaluated only the cytoplasmic TXNIP expression in relation of tumour the progression.

Correlation analysis. The TXNIP expression in tumour cells was significantly correlated with tumour size, grade and T-classification and tumour necrosis as well as postoperative progression of cRCCs (Table 1, all $p < 0.001$). Kaplan–Meier analysis revealed that patients having a cRCC with cytoplasmic expression of TXNIP protein have a significantly shorter disease-free survival compared to those without TXNIP expression (Fig. 3A). Univariate Cox regression analysis revealed that tumor size, grade, T classification, necrosis as well as cytoplasmic TXNIP positivity were significantly associated with postoperative tumour progression (all $p < 0.001$). However, in multivariate Cox regression analysis only cytoplasmic TXNIP expression and necrosis remained independent predictor of cancer progression indicating two times higher risk of postoperative tumour relapse (Table 2). Kaplan–Meier analysis showed that patients having a cRCC without cytoplasmic expression of IL1 β protein have a shorter disease-free survival compared to those with cytoplasmic IL1 β expression (Fig. 3B). In multivariate cox regression analysis no correlation between IL1 β expression and postoperative relapse has been found. IL1 β protein level showed a significant correlation only with histological grade ($p < 0.05$).

Discussion

We analysed the expression of TXNIP protein in a large cohort of cRCC without detectable metastasis at the time of operation. The Kaplan–Meier survival analysis indicated that patients with tumours displaying cytoplasmic TXNIP protein expression have significantly shorter tumour free survival ($p < 0.001$). Multivariate analysis revealed that these patients have a more than two times higher risk to develop a metastatic disease during the median follow-up of 73 months ($p = 0.001$).

The only report on TXNIP and renal cancer evaluated RNA expression data deposited in Cancer Genome Atlas (TCGA) and concluded that decreased expression of TXNIP predicts a poor prognosis³¹. Reduced expression or lack of expression of TXNIP was associated with the development of oxidative stress induced experimental RCC in rat²⁹. Decrease of TXNIP RNA in bladder cancer and development of bladder cancer in TXNIP-KO mice has been described²⁷. Low expression of TXNIP was observed in high grade glioma tissues by comparing

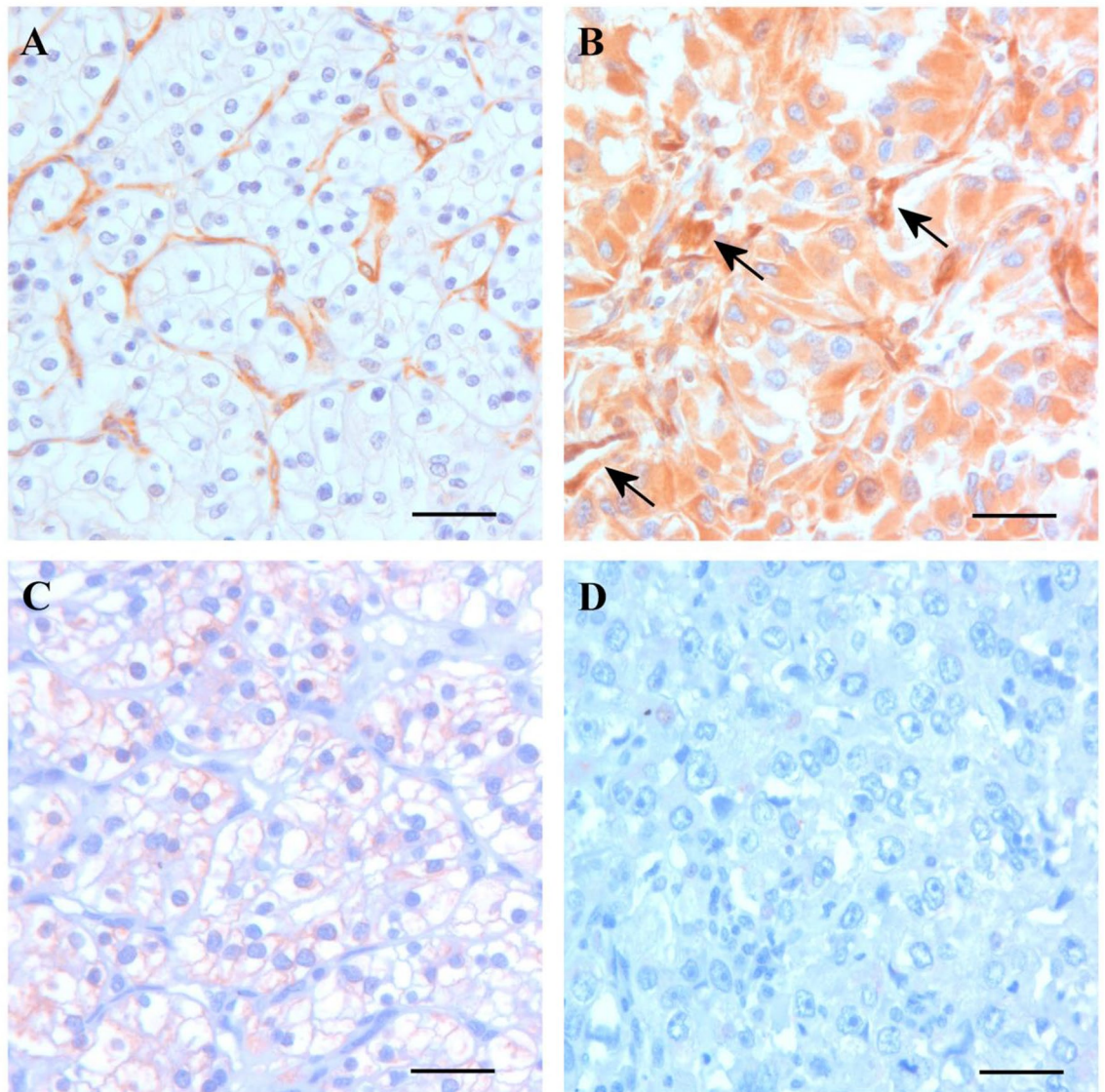


Figure 1. Expression of TXNIP and IL1 β in the two groups of conventional RCC. (A) No cytoplasmic TXNIP expression was detected in the first group of tumours of excellent prognosis. Endothelial cells of the fine vascular network display TXNIP positivity. (B) Tumour of the second group with poor prognosis display strong cytoplasmic TXNIP expression and contains few tortuous vessels (arrows). (C) Grade 1 tumour of the first group displaying cytoplasmic IL1 β expression. (D) Grade 2 tumour of the second group without IL1 β immunostaining. No IL1 β expression can be seen in the tumour microenvironment. Scale bar: 40 μ m.

to low grade tumours²⁵. In experimental mouse model the silencing of TXNIP increased the predisposition to hepatocellular carcinoma (HCC)³⁰. In two studies expression of TXNIP was detected in all of primary human HCC, but the expression was decreased in 66% and 50% of the cases, respectively^{28,32}. Based on these data TXNIP was suggested to be a tumour suppressor gene. However, in line with our results a significantly increased expression of TXNIP and elevated ROS level was associated with invasive growth in human hepatocellular carcinoma and high expression of TXNIP was an independent prognostic factor in non-small lung cancer^{22,23}.

TXNIP is a member of α -arrestin protein family and by directly binding to the antioxidant TXN blocks its reducing potential¹³. TRXs are small redox active proteins that play an important role to maintain the cellular redox balance under normal conditions. Elevated TXNIP expression and oxidative stress influence several biological functions, regulates cell growth, differentiation and apoptosis^{33,34}. By supporting the ROS production TXNIP promotes endothelial cells proliferation and angiogenesis by activating the transcription factor NF- κ B and regulating the vascular endothelial growth factor (VEGF), and vascular endothelial growth factor receptor 2 (VEGFR2) signalling^{18,35,36}. The importance of TXNIP in the maintenance of endothelial homeostasis was recently demonstrated by a TXNIP-KO mouse experiment³⁷. ROS are also involved in the induction of HIF family transcription factors the major signalling components downstream of hypoxia³⁸. Many of the HIF target proteins are also involved in the angiogenesis. In our study no HIF1 α expression has been observed the tumours cells.

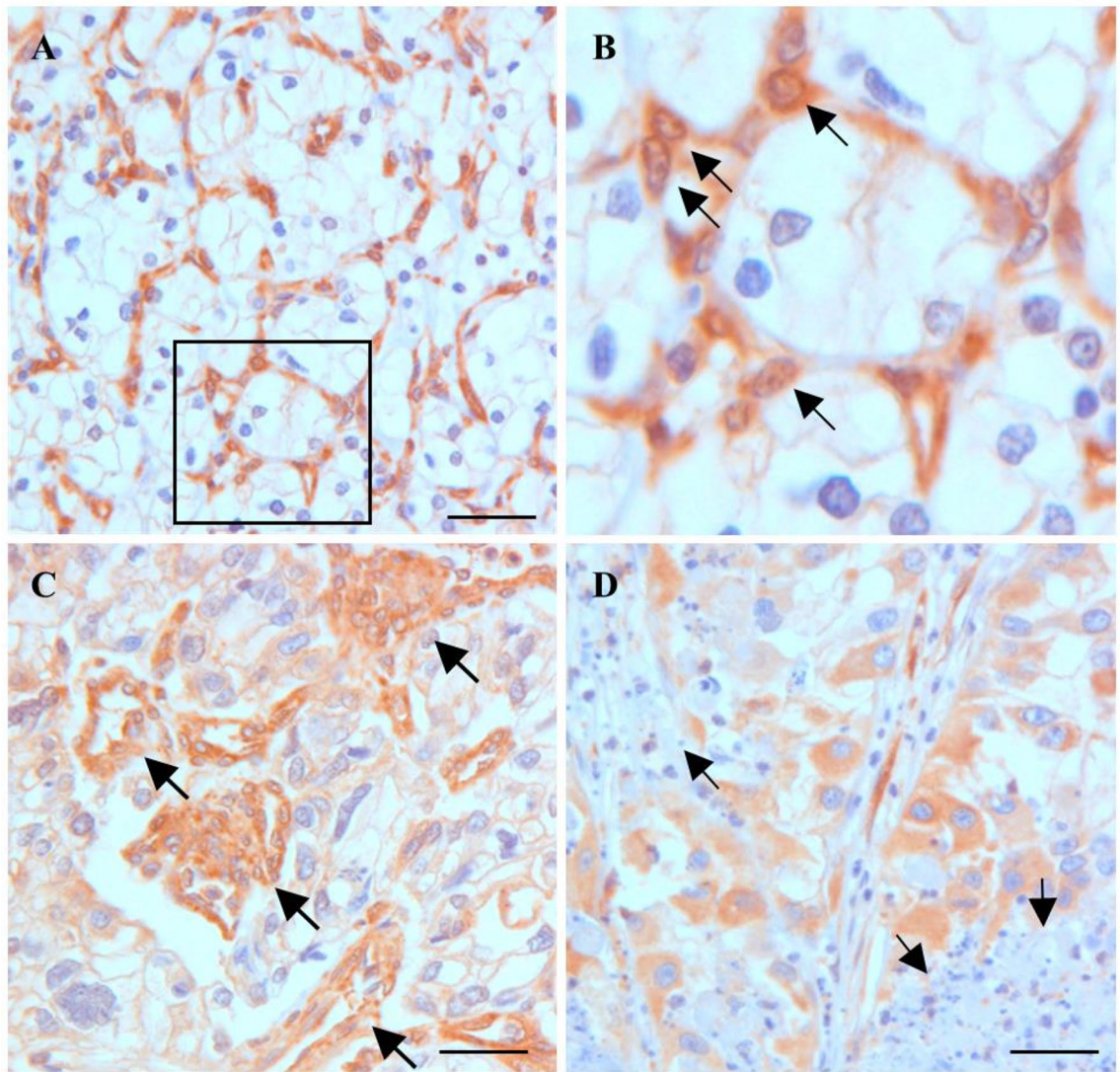


Figure 2. Expression of TXNIP in conventional RCC. (A) Strong TXNIP staining in endothelial cells but lack of expression in tumour cells. (B) Enlargement of the insert from A shows TXNIP translocation into endothelial cell nuclei (arrows). (C) Irregular tortuously growing TXNIP positive vessels in a grade 3 conventional RCC (arrows). (D) Small necrotic tumour areas are surrounded by tumour cells showing high expression of TXNIP protein (arrows). Scale bar: 40 μ m.

We showed in this study that slowly growing, differentiated cRCC with excellent clinical outcome displays an organized vascular network consisting of TXNIP positive endothelial cells. The translocation of TXNIP into the nuclei of endothelial cells of tumour supporting vessels indicates an increased level of ROS. It was shown previously that forced expression of TXNIP in isolated microvascular endothelial cells results in its nuclear translocation and activates the NF- κ B pathway leading to expression of pro-inflammatory cytokines including IL1 β ^{20,39,40}. Based on our results that IL1 β expressed preferentially in a group of tumours showing strong TXNIP nuclear expression in supporting endothelial cells indicates that the IL1 β expression is mediated through the NF κ B pathway, rather than direct activation of NLRP3 inflammasome. Recently, it was shown that IL1 β mediates epithelial to mesenchymal transition of proximal tubular cells of kidney²¹. Conventional RCC derives from proximal tubular cells of the kidney. However, we found IL1 β expression in the group of cRCC, with excellent outcome of disease and not in the group of tumours with increased cell motility leading to high risk of postoperative metastatic growth.

We showed in this study that rapid growth of tumour cells in highly malignant cRCC with metastatic capacity exceeded the proliferation of oxygen supplying capillaries. The tumour cell/blood vessel relation is strongly shifted in favour of tumour cells and lead to inefficient vascularisation by unorganized and tortuous vessels. Elevated ROS level can impair the function of important proteins and interfere with metabolic pathways. In hypoxic microenvironment the ATP is mostly produced via high rate of anaerobic glycolysis and the Warburg effect leads to lactic acid fermentation and further increases oxidative stress^{41,42}. The hypoxic and acidic TME may dramatically change the oxidative-reductive balance by producing high level of ROS which in increased concentration may inhibit tumour growth⁴³⁻⁴⁵. The high level of oxidative stress may cause serious damage of

	Nr of cases (691)	TXNIP expression		<i>p</i> -value
		Negative (512)	Positive (179)	
Gender				0.001
Male	406	282	124	
Female	285	230	55	
Status				<0.001
AWD	579	465	114	
PTR	112	47	65	
Size				0.001
< 4 cm	272	220	52	
4 < x < 7 cm	269	196	73	
> 7 cm	150	96	54	
T Stadium				<0.001
pT1	511	401	110	
pT2	94	66	28	
pT3	86	45	41	
Grade				<0.001
G1	456	382	74	
G2	180	114	66	
G3	55	16	39	
Necrosis				<0.001
No	608	479	129	
Yes	83	33	50	
Stage				<0.001
I	504	397	107	
II	167	104	63	
III	20	11	9	

Table 1. Association of TXNIP expression with clinical-pathological parameters of conventional RCCs without metastasis at the time of operation (n = 691). AWD alive without disease, PTR postoperative tumour relapse.

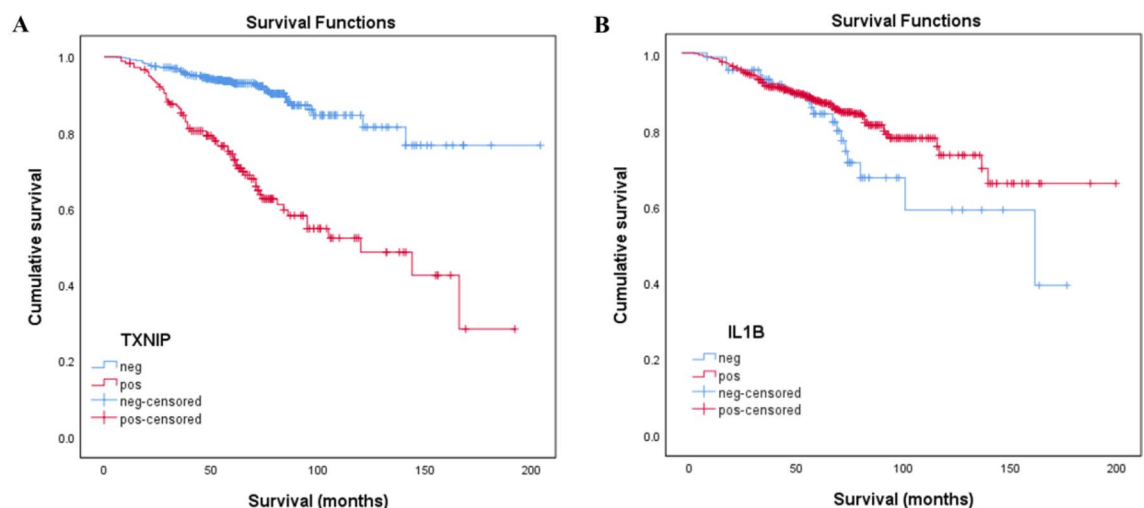


Figure 3. Kaplan–Meier estimates for disease free survival for 691 patients without metastatic disease at the time of operation. (A) Positive cytoplasmic immunostaining of TXNIP protein indicates its prognostic value ($p < 0.001$). (B) Although, cytoplasmic positivity of IL1 β indicates a better outcome of the disease, it is not significant ($p = 0.109$).

	RR	95.0% CI for Exp(B)		p-value
		Lower	Upper	
Gender				
Male/female	0.880	0.587	1.321	0.538
Size (cm)				
< 4				0.178
4 < x < 7	1.246	0.636	2.441	0.521
> 7	0.767	0.334	1.758	0.531
T Stadium				
pT1				0.002
pT2	2.553	0.304	21.457	0.388
pT3	5.976	0.768	46.480	0.088
Grade				
G1				0.062
G2	1.655	0.982	2.788	0.059
G3	2.102	1.120	3.944	0.021
Necrosis				
No/yes	1.928	1.241	2.997	0.004
Stage				
I				0.884
II	1.680	0.212	13.334	0.624
III	1.654	0.219	12.486	0.626
TXNIP				
Cytoplasmic neg/pos	2.034	1.334	3.102	0.001

Table 2. Multivariate analysis of positive TXNIP expression in 691 conventional RCCs.

tumour DNA and proteins leading to death of cancer cells⁴⁶. We showed in this study that the highest expression of TXNIP protein occurred in tumour areas with small circumscribed tumour cell necrosis. In multivariate analysis, in addition to TXNIP positivity, tumour necrosis was presented as independent prognostic factor of postoperative tumour relapse ($p = 0.004$).

In conclusion, our current study demonstrates that cRCC displaying a fine organised capillary network with nuclear translocation of TXNIP and expressing IL1 β have a good prognosis. In contrary, we showed a significant correlation between cytoplasmic TXNIP expression, inefficient vascularisation by unorganized and tortuous vessels causing tumour cell necrosis and postoperative tumour relapse of cRCC.

Material and methods

Patients. We have analysed a cohort of cRCCs obtained from 691 patients operated between 2000 and 2013 without clinically detectable metastasis at the first observation described previously⁴⁷. Data on regular follow-up and tumour specific death was obtained from Tumour Registry of the Department of Urology in accordance with the relevant institutional guidelines and regulations. Follow-up was defined as a time from the operation until the last recorded control or cancer specific death. The pertinent clinical and pathological data in are presented in Table 1. Of the 691 patients, 406 (59%) were males and 285 (41%) females, the mean age of the cohort was 61.3 ± 11.2 years (range 23–88 years). The average tumour size was 50.2 ± 25.8 mm. During the median follow-up of 73 ± 28 months, tumour relapse was observed in 112 patients (16%). Of 691 tumours, 511 (74%) were classified as pT1 including 308 (45%) pT1a tumour. The overwhelming majority of cRCCs (456 of 691) displayed G1 tumour grade. Regarding to the tumour stage, 671 (97%) of tumours were designed to stage I and II.

Tumour samples and tissue microarray (TMA). The histological diagnosis and TNM classification was established by a genitourinary pathologist (GK) according to the Heidelberg and TNM classification and by applying 3 trier grading^{48,49}. The collection and use of all tissue samples for this study was approved by the Ethics Committee of the University Pecs, Hungary (No. 5343/2014). All participants sign an informed consent that after establishing the histological diagnosis the rest of formalin fixed and paraffin embedded material can be used for immunohistochemistry. We have identified representative tumour areas on haematoxylin and eosin stained slides and the corresponding paraffin blocks were used for TMA construction. Three to five core biopsies with a diameter of 0.6 mm were taken from each tumour and were placed in the recipient block using a Manual Tissue Arrayer (MTA1, Beecher Instruments, Inc., Sun Prairie, USA). We have also analysed foetal and adult kidneys for establishing the TXNIP, HIF1 α and IL1 β expression in normal renal tissue.

Immunohistochemistry. After removing the paraffin and rehydration the 4 μ m thick sections were subjected to heat-induced epitope retrieval in citrate buffer, pH 6.0 for IL1 β and EnVision FLEX Target Retrieval

Solution, high pH (DAKO, Glostrup, Denmark) for TXNIP and HIF1 α in 2100-Retriever (Pick-Cell Laboratories, Amsterdam, The Netherlands). Endogenous peroxidase was blocked with Envision FLEX Peroxydase Blocking Reagent (DAKO) for 10 min at room temperature. Slides were then incubated at room temperature for one hour with monoclonal rabbit anti-TXNIP antibody (EPR14774, ab 188865, abcam, Cambridge, UK) at the dilution of 1:200; monoclonal mouse interleukin 1 beta antibody (AM06692SU-N, Origene Rockville, MD, USA) at the dilution of 1:200; and monoclonal rabbit anti HIF-1 alpha antibody (EP1215Y, abcam, UK) at the dilution of 1:600. EnVision FLEX horse-radish-peroxydase conjugated secondary antibody (DAKO) was applied for 30 min at room temperature and colour was developed using the DAB substrate (DAKO). Tissue sections were counterstained with Mayer's haematoxylin (Lillie's modification, DAKO) and after 10 s bluing were mounted with Pertex. For negative control the primary antibody was omitted and for positive control we used the normal kidney biopsies included into the TMAs. We have scored the TXNIP staining as negative, medium and high expression. If at least one of the 3 or more core biopsies was positive, we evaluated the tumour as positive.

Statistical analysis. Statistical analysis was carried out as described earlier⁴⁷. Correlations between categorical variables were estimated with Fisher's exact test. Estimates of the cumulative survival distributions were calculated by the Kaplan–Meier method, and the differences between the groups were compared using the log-rank test. The significance of clinical-pathological variables was evaluated using the univariate and multivariate Cox proportional hazard regression model. Analysis was performed using IBM SPSS Statistics v.27 for Windows (Inc. Chicago IL, USA). *p*-value < 0.05 was considered the limit of statistical significance.

Data availability

The datasets are available from the corresponding authors on reasonable request.

Received: 20 October 2020; Accepted: 28 June 2021

Published online: 25 August 2021

References

1. Ferlay, J. *et al.* Cancer incidence and mortality patterns in Europe: Estimates for 40 countries in 2012. *Eur. J. Cancer* **49**, 1374–1403 (2013).
2. Levi, F. *et al.* The changing pattern of kidney cancer incidence and mortality in Europe. *BJU Int.* **101**, 949–958 (2008).
3. Chow, W. U. *et al.* Epidemiology and risk factors for kidney cancer. *Nat. Rev. Urol.* **7**, 245–257 (2010).
4. Harada, K. *et al.* Acquired resistance to Temozolomide in human renal carcinoma cells is mediated by the constitutive activation of signal transduction pathways through mTORC2. *Br. J. Cancer* **109**, 2389–2395 (2013).
5. Kanesvaran, R. *et al.* Targeted therapy for renal cell carcinoma: the next lap. *Carcinogenesis* **13**, 3 (2014).
6. Balkwill, F. R. *et al.* Tumor microenvironment at a glance. *J. Cell Sci.* **125**, 5591–5596 (2012).
7. Wang, M. *et al.* Role of tumor microenvironment in tumorigenesis. *J. Cancer* **8**, 761–773 (2017).
8. Hanahan, D. *et al.* Hallmarks of cancer: The next generation. *Cell* **144**, 646–674 (2011).
9. Policastro, L. L. *et al.* The tumor microenvironment characterization, redox considerations, and novel approaches for reactive oxygen species-targeted therapy. *Antioxid. Redox Signal* **19**, 854–895 (2013).
10. Gajewski, T. F. *et al.* Innate and adaptive immune cells in the tumor microenvironment. *Nat. Immunol.* **14**, 1014–1022 (2013).
11. Sauer, H. *et al.* Reactive oxygen species as intracellular messengers during cell growth and differentiation. *Cell Physiol. Biochem.* **22**, 173–186 (2001).
12. Quinn, M. T. *et al.* The expanding role of NADPH oxidases in health and disease: No longer just agents of death and destruction. *Clin. Sci. (Lond)* **111**, 1–20 (2006).
13. Ushio-Fukai, M. *et al.* Reactive oxygen species and angiogenesis: NADPH oxidase as target for cancer therapy. *Cancer Lett.* **266**, 37–52 (2008).
14. Li, Q. *et al.* NADPH oxidase subunit p22(phox)-mediated reactive oxygen species contribute to angiogenesis and tumor growth through AKT and ERK1/2 signaling pathways in prostate cancer. *Biochim. Biophys. Acta* **1833**, 3375–3385 (2013).
15. Jung, S. N. *et al.* Reactive oxygen species stabilize hypoxia-inducible factor-1 alpha protein and stimulate transcriptional activity via AMP-activated protein kinase in DU145 human prostate cancer cells. *Carcinogenesis* **29**, 713–721 (2008).
16. Nishiyama, A. *et al.* Identification of thioredoxin-binding protein-2/vitamin D3 up-regulated protein 1 as a negative regulator of thioredoxin function and expression. *J. Biol. Chem.* **274**, 21645–21650 (1999).
17. Abdelsaid, M. *et al.* Thioredoxin-interacting protein expression is required for VEGF-mediated angiogenic signal in endothelial cells. *Antioxidants Redox Signal.* **19**, 2199–2212 (2013).
18. Colavitti, R. *et al.* Reactive oxygen species as downstream mediators of angiogenic signaling by vascular endothelial growth factor receptor-2/KDR. *J. Biol. Chem.* **277**, 3101–3108 (2002).
19. Zhou, R. *et al.* Thioredoxin-interacting protein links oxidative stress to inflammasome activation. *Nat. Immunol.* **11**, 136–140 (2010).
20. Mohamed, I. N. *et al.* Role of inflammasome activation in the pathophysiology of vascular diseases of the neurovascular unit. *Antioxidants Redox Sign.* **22**, 1188–1206 (2015).
21. Masola, V. *et al.* In vitro effects of interleukin (IL)-1 beta inhibition on the epithelial-to-mesenchymal transition (EMT) of renal tubular and hepatic stellate cells. *J. Transl. Med.* **17**, 12 (2019).
22. Gunes, A. *et al.* Thioredoxin interacting protein promotes invasion in hepatocellular carcinoma. *Oncotarget* **9**, 36849–36868 (2018).
23. Li, Y. *et al.* Hypoxia induced high expression of thioredoxin interacting protein (TXNIP) in non-small cell lung cancer and its prognostic effect. *Asian Pac. J. Cancer Prev* **16**, 2953–2958 (2015).
24. Morrison, J. A. *et al.* Thioredoxin interacting protein (TXNIP) is a novel tumor suppressor in thyroid cancer. *Mol. Cancer* **13**, 62 (2014).
25. Zhang, P. *et al.* A novel indication of thioredoxin-interacting protein as a tumor suppressor gene in malignant glioma. *Oncol. Lett.* **14**, 2053–2058 (2017).
26. Jiao, D. *et al.* UHRF1 promotes renal cell carcinoma progression through epigenetic regulation of TXNIP. *Oncogene* **38**, 5686–5699 (2019).
27. Nishizawa, K. *et al.* Thioredoxin-interacting protein suppresses bladder carcinogenesis. *Carcinogenesis* **32**, 1459–1466 (2011).
28. Kwon, H. J. *et al.* Vitamin D3 upregulated protein 1 suppresses TNF-alpha-induced NF-kappaB activation in hepatocarcinogenesis. *J. Immunol.* **185**, 3980–3989 (2010).

29. Dutta, K. K. *et al.* Two distinct mechanisms for loss of thioredoxin-binding protein-2 in oxidative stress-induced renal carcinogenesis. *Lab. Invest.* **85**, 798–807 (2005).
30. Sheth, S. S. *et al.* Hepatocellular carcinoma in TXNIP-deficient mice. *Oncogene* **25**, 3528–3536 (2006).
31. Gao, Y. *et al.* Decreased expression of TXNIP predicts poor prognosis in patients with clear cell renal cell carcinoma. *Oncol. Lett.* **19**, 763–770 (2020).
32. Li, J. *et al.* TXNIP overexpression suppresses proliferation and induces apoptosis in SMMC7221 cells through ROS generation and MAPK pathway activation. *Oncol. Rep.* **37**, 3369–3376 (2017).
33. Masutani, H. *et al.* Thioredoxin binding protein (TBP)-2/Txnip and a-arrestin proteins in cancer and diabetes mellitus. *J. Clin. Biochem. Nutr.* **50**, 23–34 (2012).
34. Zhou, J. B. *et al.* Roles of thioredoxin-binding protein (TXNIP) in oxidative stress, apoptosis and cancer. *Mitochondrion* **13**, 163–169 (2013).
35. Dunn, L. L. *et al.* A critical role of thioredoxin-interacting protein in diabetes-related impairment of angiogenesis. *Diabetes* **63**, 675–687 (2014).
36. González-Pacheco, F. R. *et al.* Mechanism of endothelial response to oxidative aggression: protective role of autologous VEGF and induction of VEGFR2 by H₂O₂. *Am. J. Physiol. Circ. Physiol.* **291**, H1395–1401 (2006).
37. Domingues, A. *et al.* Targeting endothelial thioredoxin-interacting protein (TXNIP) protects from metabolic disorder-related impairment of vascular function and post-ischemic revascularisation. *Angiogenesis* **23**, 249–264 (2020).
38. Kietzmann, T. *et al.* Reactive oxygen species in the control of hypoxia-inducible factor-mediated gene expression. *Semin. Cell Dev. Biol.* **16**, 474–486 (2005).
39. Perrone, L. *et al.* Thioredoxin interacting protein (TXNIP) induces inflammation through chromatin modification in retinal capillary endothelial cells under diabetic condition. *J. Cell Physiol.* **221**, 262–272 (2009).
40. Perrone, L. *et al.* Inhibition of TXNIP expression in vivo blocks early pathologies of diabetic nephropathy. *Cell Death Dis.* **1**, e65 (2010).
41. Van der Heiden, M. G. *et al.* Understanding the Warburg effect: the metabolic requirements of cell proliferation. *Science* **324**, 1029–1033 (2009).
42. Mitsuishi, Y. *et al.* Nrf2 redirects glucose and glutamin into anabolic pathways in metabolic reprogramming. *Cancer Cell* **22**, 66–79 (2012).
43. Chang, C. L. *et al.* Oxidative stress inactivates the human DNA mismatch repair system. *Am. J. Physiol. Cell Physiol.* **283**, C148–154 (2002).
44. Le Jan, S. *et al.* Characterisation of the expression of the hypoxia-induced genes neuritin, TXNIP and IGFBP3 in cancer. *FEBS Lett.* **580**, 3395–3400 (2006).
45. Shen, H. M. *et al.* TNF receptor superfamily-induced cell death: redox-dependent execution. *FASEB J.* **20**, 1589–1598 (2006).
46. Morgan, M. J. *et al.* TNF α and reactive oxygen species in necrotic cell death. *Cell Res.* **18**, 343–349 (2008).
47. Peterfi, L. *et al.* Expression of RARRES1 and AGBL2 and progression of conventional renal cell carcinoma. *Brit. J. Cancer* **122**, 1818–1824 (2020).
48. Kovacs, G. *et al.* The Heidelberg classification of renal cell tumours. *J. Pathol.* **183**, 131–133 (1997).
49. Brierley, J. *et al.* *TNM Classification of Malignant Tumours* (Wiley, 2017).

Acknowledgements

This study is supported by a grant of the Medical Faculty of the University of Pecs, Hungary (PTE AOK KA 2019/41) to DB.

Author contributions

G.K. and D.B. contributed to study concept and design. G.K. carried out the pathological analysis and constructed the TMA. M.M. and L.P. made the immunohistochemistry, L.D. and M.Y. made the data and statistical analysis. M.M. and D.B. wrote the first draft and G.K. reviewed the manuscript. All authors read and approved the final version of the manuscript submitted for publication.

Competing interests

The authors declare no competing interests.

Additional information

Correspondence and requests for materials should be addressed to G.K.

Reprints and permissions information is available at www.nature.com/reprints.

Publisher's note Springer Nature remains neutral with regard to jurisdictional claims in published maps and institutional affiliations.



Open Access This article is licensed under a Creative Commons Attribution 4.0 International License, which permits use, sharing, adaptation, distribution and reproduction in any medium or format, as long as you give appropriate credit to the original author(s) and the source, provide a link to the Creative Commons licence, and indicate if changes were made. The images or other third party material in this article are included in the article's Creative Commons licence, unless indicated otherwise in a credit line to the material. If material is not included in the article's Creative Commons licence and your intended use is not permitted by statutory regulation or exceeds the permitted use, you will need to obtain permission directly from the copyright holder. To view a copy of this licence, visit <http://creativecommons.org/licenses/by/4.0/>.

© The Author(s) 2021